Hurlbert, R. B., Schmitz, H., Brumm, A. F., and Potter, V. R. (1954), *J. Biol. Chem. 209,* 23.
Lane, B. G., and Tamaoki, T. (1969), *Biochim. Biophys. Acta 179,* 332.
Liau, M. C. (1974), *Fed. Proc., Fed. Amer. Soc. Exp. Biol. 33,* 1583.
Liau, M. C., Craig, N. C., and Perry, R. P. (1968), *Biochim. Biophys. Acta 169,* 196.
Liau, M. C., Flatt, N. C., and Hurlbert, R. B. (1970), *Biochim. Biophys. Acta 224,* 282.
Liau, M. C., Hnilica, L. S., and Hurlbert, R. B. (1965), *Proc. Nat. Acad. Sci. U. S. 53,* 626.
Liau, M. C., Hunt, J. B., Smith, D. W., and Hurlbert, R. B. (1973), *Cancer Res. 33,* 323.
Liau, M. C., O'Rourke, C. M., and Hurlbert, R. B. (1972), *Biochemistry 11,* 629.
Miller, E. G., and Hurlbert, R. B. (1969), *J. Cell Biol. 43,* 93a.
Muramatsu, M., and Fujisawa, T. (1968), *Biochim. Biophys. Acta 157,* 476.
Petermann, M. L., and Pavlovec, A. (1963), *J. Biol. Chem. 238,* 318.
Salim, M., and Maden, B. E. H. (1973), *Nature (London) 244,* 334.
Sneider, T. W. (1971), *J. Biol. Chem. 246,* 4774.
Srinivasan, P. R., and Borek, E. (1963), *Proc. Nat. Acad. Sci. U. S. 49,* 529.
Tamaoki, T., and Lane, B. G. (1968), *Biochemistry 7,* 3431.
Vande Woude, G. F., Polatnick, J., and Ascione, R. (1970), *J. Virol. 5,* 458.
Vaughan, M. H., Soeiro, R., Warner, J. R., and Darnell, J. E. (1967), *Proc. Nat. Acad. Sci. U. S. 58,* 1527.
Wagner, E., Penman, S., and Ingram, V. (1967), *J. Mol. Biol. 29,* 371.
Weinberg, R. A., Loening, U., Willems, M., and Penman, S. (1967), *Proc. Nat. Acad. Sci. U. S. 58,* 1088.
Zimmerman, E. F. (1968), *Biochemistry 7,* 3156.
Zimmerman, E. F., and Holler, B. W. (1967), *J. Mol. Biol. 23,* 149.

Hydrodynamic Diameters of RNA Tumor Viruses. Studies by Laser Beat Frequency Light Scattering Spectroscopy of Avian Myeloblastosis and Rauscher Murine Leukemia Viruses†

I. Salmeen,* L. Rimai, L. Liebes, M. A. Rich, and J. J. McCormick

ABSTRACT: The diffusion constants of avian myeloblastosis virus (AMV) and murine leukemia virus (MuLV) (Rauscher) suspensions in buffer and in 30% sucrose were determined by laser beat frequency light scattering spectroscopy at a series of temperatures ranging from 5 to 25°. By the use of the Stokes–Einstein equation, the following hydrodynamic diameters are calculated at 20°: MuLV, 154 ± 3 nm in sucrose and 145 ± 7 nm in buffer; AMV, 144 ± 3 nm in sucrose and 138 ± 4 nm in buffer. While the diameters measured in buffer were temperature independent, the diameters measured in sucrose decreased by about 20% as the temperature was raised from 5 to 25°. The concentration of virus particles in the suspensions ranged from 10^7 to 10^9 particles/ml. The absolute particle concentrations are estimated within ±30% by determining the dilution needed to reach a concentration sufficiently low that the particle number fluctuation contribution was comparable to that of the interference scattering. Particle weights of 3.9×10^8 daltons for MuLV and 4.0×10^8 daltons for AMV were calculated from the diffusion constants and from our own experimentally determined sedimentation coefficients. From these particle weights and the hydrodynamic diameters of the viruses, we calculated the per cent of the hydrodynamic volume of the viruses which could be freely penetrated by water, *viz.*, 57% for AMV and 69% for MuLV.

Avian myeloblastosis virus (AMV)[1] and murine leukemia virus (MuLV) are widely used as typical representatives of oncornaviruses in investigations of the pathology of virus-induced animal tumors, the mode of infection, replication and transformation, and in the characterization of the viruses (Temin, 1971). While oncornaviruses have been etiologically associated with leukemias and sarcomas in mice, chickens, and other animals including some higher primates, their role in human cancer has not yet been unequivocally demonstrated. AMV and MuLV have been particularly useful since they are present at relatively high titers in the plasma of viremic animals and thus permit purification of sufficient quantities for physical and biochemical characterization.

Oncornaviruses are generally spherical in shape with diameter estimates ranging from 65 to 150 nm (Bader, 1969). As observed in electron micrographs, they contain an electron dense core positioned either centrally (C type particles)

† From the Scientific Research Staff, Ford Motor Company, Dearborn, Michigan 48121 (I.S. and L.R.) and the Michigan Cancer Foundation, Detroit, Michigan 48201 (L.L., M.A.R., and J.J.McC.). *Received July 11, 1974.* This research was supported by U.S. Public Health Service, National Institutes of Health, Contracts NOI-CP-33226 and NOI-CP-33347 and Grants CA-13058 and CA-14680, and by an institutional grant to the Michigan Cancer Foundation by the United Foundation of Greater Detroit.

[1] Abbreviations used are: AMV, avian myeloblastosis virus; MuLV, murine leukemia virus.

or eccentrically (B type particles). The core, with a diameter of *ca.* 80 nm, contains the viral genome in the form of one high molecular weight RNA molecule (10^7), various smaller RNA molecules, some low molecular weight DNA, the enzyme reverse transcriptase, and a number of other proteins (Temin, 1971). Ultracentrifugation studies on AMV (Sharp and Beard, 1954) and MuLV (Mora *et al.*, 1966) yield sedimentation coefficients of 693 S and 640 S, respectively. The AMV and MuLV particle weights have been reported as 7.5×10^{-13} (Bonar and Beard, 1959) and 3.6×10^{-13} mg, respectively (Mora *et al.*, 1966). Since these viruses are formed by budding from the surface of infected vertebrate cells, they retain the modified cell membrane. The composition of AMV has recently been estimated as 61.5% protein, 36.1% lipid, and 21.4% RNA (Stromberg *et al.*, 1973); similar compositions are thought to obtain for other oncornaviruses.

The study of the role of oncornaviruses in the etiology of animal cancers and, perhaps, of human cancers, requires physical methods for rapidly and nondestructively quantitating and characterizing virus particles. For the size and available concentration range of these viruses, light scattering is one of the most sensitive physical techniques since the wavelength of visible radiation is comparable to the dimensions of viral particles. Light scattering, as it has been commonly used in macromolecular characterization, has been based on measurements of the time averaged intensity of the scattered light (Rayleigh scattering) (Tanford, 1961). In contrast, the recently developed technique of laser beat frequency light scattering spectroscopy (also called quasi-elastic scattering, intensity fluctuation spectroscopy, and optical mixing spectroscopy) is based on an analysis of the time dependence of the scattered intensity (Benedek, 1968; Clark *et al.*, 1970; Pusey *et al.*, 1974). This time dependence is due to the Brownian motion of particles in solution and, for a monodisperse suspension of spherical particles, can be analyzed to yield the diffusion constant and an estimate of the particle concentration (Schaefer and Berne, 1972). Laser beat frequency spectroscopy has been used previously for the study of proteins, viruses, bacteriophages, red blood cells, and bacterial motility (Dubin *et al.*, 1971; Salmeen *et al.*, 1972; Camerini-Otero *et al.*, 1974).

In this study, we have measured the diffusion constants of AMV and MuLV suspended in *ca.* 30% sucrose and in sucrose-free buffers over the temperature range 5–25°. The particle concentrations, as determined in these light scattering experiments, were in the range 1×10^7 to 10^9 particles/ml. Measurements at three scattering angles of samples with *ca.* 10^8 particles/ml required about 10 min. With these diffusion constants we calculated the hydrodynamic diameters, assuming that the particles are spherical and that the Stokes–Einstein equation relating the diffusion constant with viscosity and particle diameter is valid. We also used these diffusion constants together with our own experimentally determined values for the sedimentation coefficients to calculate particle weights. From the particle weights and the hydrodynamic diameters, the volume of the viruses which can be penetrated freely by water is estimated (this water should be distinguished from that which is bound by specific interactions [see, for example, Harrison, 1969]). We also tested the feasibility of directly studying, by this technique, viruses in body fluids.

Light Scattering Theory

The theory of laser beat frequency spectroscopy has been reviewed most recently by Pusey *et al.* (1974) (see also Benedek, 1968; Clark *et al.*, 1970). In the following we present only the essentials necessary for understanding the results.

Under the conditions of the present experiments, the scattering from the solvent is negligible compared with that from the virus particles. Thus, at the detector (photomultiplier tube) the electric field is the sum of the fields scattered by the individual particles. Since the output photocurrent of the photomultiplier is proportional to the square of the incident electric field, the photocurrent will be proportional to the square of the sum of the contributions to the scattered field from all particles within the scattering volume. Thus, the photocurrent will contain interference terms which will cause the observed scattering to be dependent on scattering angle.

Since the particles undergo Brownian motion, the scattered intensity will consist of time dependent terms in addition to a time independent part. The time independent term, as measured by a dc voltmeter, is the Rayleigh scattering commonly used in the study of macromolecules, and is proportional to the number of particles in the scattering volume (Tanford, 1961). This is a convenient method for monitoring relative concentrations of suspensions of the same virus. However, absolute concentrations cannot be easily determined from the Rayleigh scattering because the virus concentrations readily attainable are too low to allow measurement of the scattering efficiency of an individual virus particle. However, as discussed below, the time dependent scattering does afford a method for estimating absolute concentrations.

For the case to be considered here, two contributions to the time dependence are important. One is caused by the time fluctuations due to particle diffusion in and out of the scattering volume (Schaefer and Berne, 1972). The other is caused by the diffusion of particles within the scattering volume over distances of the order of the wavelength of light, which thus causes temporal fluctuations in the interference effect (see, for example, Clark *et al.*, 1970). The analysis of these random temporal fluctuations in photocurrent is done in terms of the autocorrelation function.

If the two time fluctuating terms are assumed to be uncorrelated with each other, then, for homodyne detection, the time autocorrelation function of the photocurrent has the form (Schaefer and Berne, 1972)

$$I(t) = \langle i(T)i(T + t)\rangle = \Gamma[N_0 e^{-\gamma t} + \beta N_0^2 e^{-2DK^2 t}] \quad (1)$$

The first term results from fluctuations in the total number of particles within the scattering volume and the second results from the diffusional interference term. N_0 is the average number of particles in the scattering volume; γ is a characteristic time required for a particle to diffuse across the scattering volume and is of the order $L^2/24N_0D$ (where L is a characteristic dimension of the scattering volume [Schaefer and Berne, 1972]); and Γ is a constant which depends on the scattering cross section. $\mathbf{K}$ is the wave vector of the spacial Fourier component of the fluctuations in polarizability which contribute to the scattering at the angle θ. $\mathbf{K} = \mathbf{K}_{\text{incident}} - \mathbf{K}_{\text{scattered}}$ where $K \approx (4\pi n/\lambda) \sin \theta/2$; λ is the vacuum wavelength of the incident light; and n is the index of refraction of the solvent.

The fluctuations in polarizability are due to corresponding fluctuations in particle concentration. $1/DK^2$ is the decay time for the component of the concentration fluctuations with wave vector $\mathbf{K}$, and is obtained directly from a so-

lution of the diffusion equation (Fick's law of diffusion [Clark *et al.*, 1970]). β is a constant (less than one) which depends on spectrometer geometry and relates the coherence length for the receiving optics to the dimensions of the scattering volume (Koppel, 1971).

Under typical experimental conditions, the decay constant of the first exponential in eq 1 is much longer than that of the second. For our spectrometer, the scattering volume is such that at 90°, $DK^2/\gamma > 100$. Thus, to a good approximation, the first term is constant during the decay time of the second. At high concentrations, the second term dominates and the experimentally observed decay constant yields the diffusion constant (see Figure 1). However, at sufficiently low concentrations, N_0 is comparable to βN_0^2, and both components contribute to the observed photocurrent correlation function (see Figure 2). Thus the ratio of the two contributions yields the absolute particle concentration, provided the constant β is known. As discussed in the Materials and Methods section, this constant can be determined experimentally from the spectrum of a dilute suspension of particles of known concentration.

The above discussion assumes a monodisperse suspension of spherical particles. For a polydisperse system eq 1 can be generalized. If the sample contains two types of particles, the correlation function (Rimai *et al.*, 1970) is

$$I(t) = \Gamma_1 N_1 e^{-\gamma_1 t} + \Gamma_2 N_2 e^{-\gamma_2 t} + \Gamma_1^2 N_1^2 e^{-2D_1 K^2 t} + \Gamma_2^2 N_2^2 e^{-2D_2 K^2 t} + \Gamma_1 \Gamma_2 N_1 N_2 e^{-(D_1+D_2)K^2 t}$$

For a continuously distributed polydisperse sample, an explicit equation can be written if the dependence of Γ on particle size is known and if a particle size distribution function can be assumed. The latter is not always possible. However, polydispersity can be recognized qualitatively by nonexponential correlation functions and by deviations from a linear dependence of the apparent decay time on $\sin^2 \theta/2$. A quantitative methodology for analyzing polydispersity has been discussed by Pusey *et al.* (1974).

Materials and Methods

a. Light Scattering Spectrometer. Light from a Spectra Physics Model 124 He–Ne laser (nominally 15 mW at 632.8 nm) is focused into the sample which is contained in a standard 5 mm × 10 mm rectangular cuvet. The cuvet holder is a three-sided double walled brass rectangular jacket through which nitrogen gas can be circulated to obtain variable temperature. The desired temperature is attained by adjusting the boil-off rate from a liquid nitrogen dewar together with the temperature of a heater through which the cold gas passes prior to reaching the jacket. The temperature is measured with a thermistor in good thermal contact with the bottom of the cuvet, but insulated from the walls of the jacket. Throughout the temperature range from 5 to 30°, the temperature stability is ±0.2°, as measured over a 15-min period. The scattered light is collected through the 10-mm face which allows data to be taken at external angles from about 60 to 120°. The scattering volume is imaged through a slit onto the photocathode of a photomultiplier tube. This tube is mounted on a rotatable arm upon which a protractor indicates the external scattering angle. The optics and diaphragms combine to produce a scattering volume of approximately 10^{-4} cm^3.

The photocurrent passes through a 100 kΩ load resistor, and, after amplification with a Tektronix Model 1A7A, the time dependent part of the voltage developed across this resistor is applied to the input of a Saicor Model SAI-42A Real Time Correlator for analysis of the time dependent scattering intensity. The instrument is used with ac coupling and in the full (nonclipped) correlation mode so that the zero output of the correlator is the true zero of the time dependent correlation function. This enables reliable correlation amplitude measurements which are important for the absolute particle number quantitation. The time-averaged voltage, which monitors the Rayleigh scattering, is measured by a Keithly Model 150A μV ammeter. Data usually were taken at three scattering angles: 70, 90, and 110° (measured externally). For a monodisperse suspension of spheres, the diffusional decay constant should be linear in $\sin^2 \theta/2$ (see eq 1). At viral concentrations of *ca.* 10^8 particles/ml, measurements at the three angles required about 10 min.

The sensitivity and accuracy of the system was checked by measuring a monodisperse dilute suspension of 176-nm diameter polystyrene latex spheres (Dow Chemical Company, 10% solids). For these spheres, the angular dependence of the decay constant was linear in $\sin^2 \theta/2$ to within 1%. From the measured diffusion constant, the diameter of the spheres was calculated using the Stokes–Einstein relation (see eq 2 in the Results section) as 175 ± 2 nm.

A dilution series of the same latex spheres, for which the concentration was determined from a dry weight analysis, together with the known density of 1.05 g/cm^3 (manufacturer's specifications), was used to check the relative intensity response of the system at 90° scattering angle and to establish the conditions under which number fluctuations measureably contribute to the observed autocorrelation function. The relative time averaged photocurrent (Rayleigh scattering) was found to be linear in concentration to within 10% over the range 10^{11}–10^7 particles/ml. At concentrations less than *ca.* 1×10^8 particles/ml, the correlation function did not decay to the zero output of the correlator, as it did at higher concentrations, but rather to a level which increased with decreasing concentration. This effect is attributed to having reached a concentration such that βN_0^2 is comparable to N_0 (see first term in eq 1). For both viruses and latex spheres, the ratio of the initial amplitude of the exponential decay to the amplitude of the background decreased linearly (to within ±30%), with decreased concentration. This ratio, along with the known concentration of latex spheres was used to estimate β. An apparent background can also be caused by large contaminating particles drifting through the scattering volume. Background caused by contamination is irreproducible. Thus, the low concentration measurements were repeated several times and the data from a sample were used only if the correlation function was reproducible to within about 30%.

Virus particle concentrations were estimated by serially diluting a virus solution to a concentration where the number fluctuations in the scattering volume measurably contributed to the autocorrelation function.

b. Glassware Cleaning. All glassware including sample cuvets were cleaned with either acid or detergent and then rinsed exhaustively with water passed through a 0.45-μ Millipore filter. The cleanliness of the cuvets was monitored by the elastic scattering of water filtered into the cuvet. "Clean" water, and hence a clean cuvet, yielded a value of less than 0.1 mV; the signal for the lowest concentration samples was of the order of 2 mV.

c. Virus Preparation. Avian myeloblastosis (BAI strain) and murine leukemia virus (Rauscher) in plasma–citrate

were generously supplied by Drs. Joseph and Dorothy Beard and University Laboratories, respectively, through the cooperation of the Virus Cancer Program of the National Cancer Institute. Virus suspensions were first subjected to a discontinuous sucrose gradient centrifugation through a 20% w/v sucrose cushion onto a 65% w/v sucrose pad (Spinco SW 50.1, rotor 98,000*g*, 1 hr). (AMV was first passed through a gauze filter and then centrifuged at 650*g* for 10 min to remove any fibrin strains prior to the ultracentrifugation step.) The viral light scattering band was collected from the bottom of the tube by employing an illuminated tube piercing apparatus (Schaffer and Fromhagen, 1965). Further purification, as noted, usually employed an additional 20–65% sucrose density gradient centrifugation (Spinco SW 27.1 rotor 130,000*g*, 12 hr).

The viral light scattering band at a density of 1.16 (0.3–0.5 ml) was collected directly from the centrifuge tube into a dust-free vial (prepared under the same criteria as described for the light scattering cuvets). The solutions were then made up to 0.02% in sodium azide with a filtered stock (0.2%) azide solution. The sucrose concentration was determined from the refractive index which was measured with a Bausch and Lomb refractometer. Laser light scattering measurements were then carried out. Subsequently, some samples, as noted in figure legends, were dialyzed overnight against three changes of either Tris–EDTA (0.005 M Tris-HCl–0.001 M EDTA (pH 8.1)) or phosphate (0.005 M phosphate (pH 7.0)) buffer. All sucrose solutions were prepared in either of these two buffers. Prior to reexamination by laser light scattering, it was found necessary to first subject the samples to a 21,000*g*, 10-min centrifugation to remove any aggregated material presumably resulting from instability of the virions during the dialysis period. Virus containing plasma citrate preparations were also subjected to the same low-speed centrifugation (21,000*g*, 10 min) prior to the light scattering measurements.

Normal mouse (*i.e.*, nonviremic) plasma–citrate preparations were prepared by a 1:1 dilution of plasma with 0.306 M sodium citrate. A reconstruction experiment in which MuLV was added to normal plasma citrate was carried out in the following manner: MuLV was sedimented from 2 ml of leukemic plasma citrate preparation (Spinco SW 50.1, 98,000*g*, 1 hr). This was resuspended into 100 μl of Tris–EDTA buffer; 50 μl of the resuspended virus was then added to 0.5 ml of normal mouse plasma–citrate. This solution was then made up to 0.02% in sodium azide as described previously. A comparison of the sample and a control plasma–citrate containing the same additions of virus free buffer was then carried out with laser light scattering. The viscosity of normal plasma–citrate was measured for us by Dr. Mikio Zinbo using a Cannon-Fenske viscometer. At 20° the viscosity of plasma–citrate is 1.23 cP and the temperature dependence is parallel to that of water.

d. Analytical Ultracentrifugation. Sedimentation velocity experiments were carried out at 20° (±0.1°) in a Spinco Model E analytical ultracentrifuge equipped with ultraviolet optics. A 12 mm, 2° Kel F centerpiece was employed. A centrifuge speed of 15,220 rpm was used with 2-min intervals between exposures for AMV and MuLV determinations. MuLV data were also obtained at a speed of 10,589 rpm using 4-min exposure intervals. Most determinations were carried out with viral preparations dialyzed against three changes of the 0.005 M, pH 7.0 phosphate buffer. A 0.005 M, pH 7.0 phosphate buffer containing 0.5 M KCl was also used. Viral concentrations of MuLV and AMV were estimated by measuring the optical density at 260 nm and then correlating this with viral particle counts previously obtained for the individual viruses from laser light scattering. All sedimentation coefficients were reduced to standard conditions (20°, water). The solvent viscosities and densities were obtained from data in the International Critical Tables. A partial specific volume, $\bar{v}$, of 0.869 for MuLV and AMV was calculated according to the method described by Markham (1967) and from the data of Stromberg *et al.* (1973) (see Results section). The sedimentation rates were determined from densitometric traces of the photographic film carried out on a Joyce-Lobel recording microdensitometer.

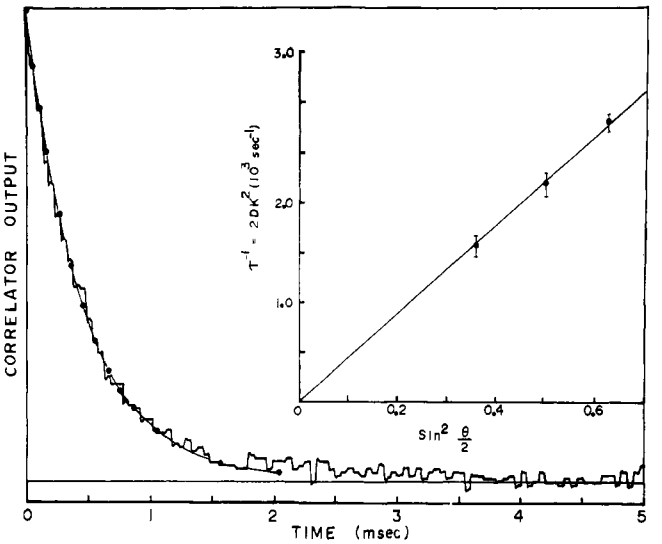

FIGURE 1: Time correlation function of scattered light intensity from a suspension of MuLV; concentration = 1.7×10^8 particles/ml in 0.005 M phosphate buffer (pH 7.0); temperature = 21.9°; scattering angle $\theta = 90°$. The base line is the zero output of the correlator. The solid dots lie on an exponential with a decay constant, $1/\tau = (2.19 \pm 0.13) = 10^3$ sec^{-1}, determined as described in the text. The angular dependence of $1/\tau$ is shown in the insert.

Results

a. Experimental Data. Figure 1 shows a typical correlation function for a sample of MuLV at a concentration of 2×10^8 particles/ml. The solid horizontal line in the figure is the base line to which the correlation function decays, and is determined by the zero output of the correlator. The solid dots lie on a calculated exponential, for which the decay constant was obtained, by the following procedure. The experimental data were assumed to be a single exponential. In such a case, the decay constant can be calculated from any pair of points. However, the noise on the experimental correlation function causes statistical fluctuations among the decay constants calculated from different pairs of points. To estimate the average decay constant, for a particular correlation function, the linear average of the decay constant determined from ten different pairs of points along the experimental curve was calculated. The root mean square deviation of this set was taken as an estimate of the statistical error for that particular correlation function. This average decay constant was used to calculate the exponential shown in the figures. This procedure was followed for each scattering angle (we used 70, 90, and 110° external angle). The average diffusion constant, or derived hydrodynamic diameter, for one particular virus sample was then taken as the linear average of the three values, one for each angle.

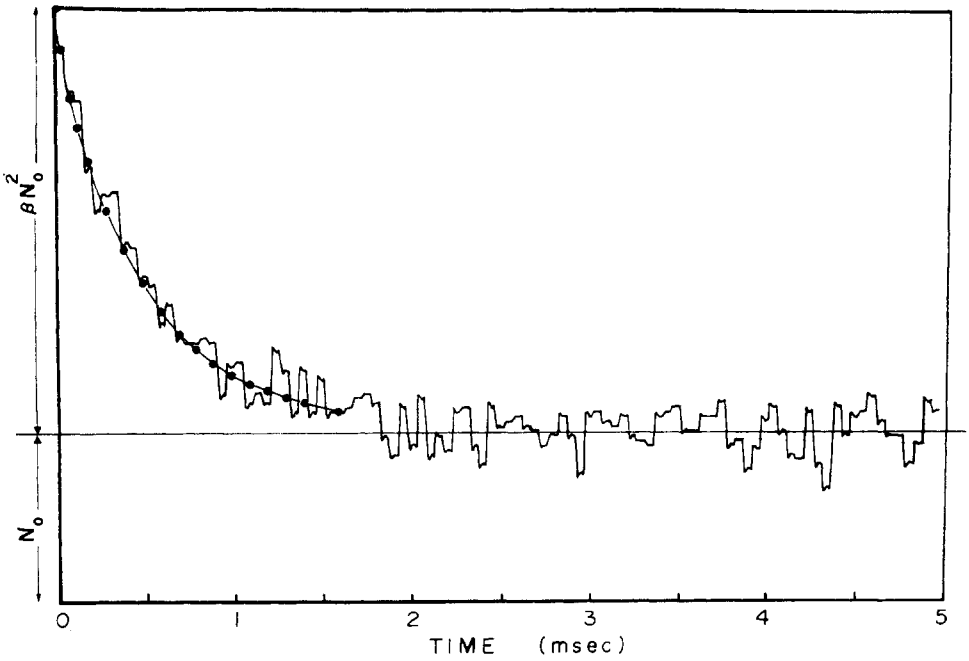

FIGURE 2: Time correlation function of scattered light intensity from a suspension of AMV; concentration = 2.2×10^7 particles/ml in 0.005 M phosphate buffer (pH 7.0); temperature = 23.2°; scattering angle $\theta = 90°$. The presence of the approximately flat base line, displaced from the correlator zero, to which the exponential decays is indicative of number fluctuations (see eq 1 in the text) expected at low concentrations. The solid dots lie on an exponential with a value of $1/\tau = (2.34 \pm 0.16) \times 10^3$ sec^{-1} estimated by the procedure described in the text.

For the data of all samples in this study, the statistical uncertainties in the decay constants of the correlation functions were in the range ±1 to ±3%. The decay constants were independent of concentration over the range 1.7×10^7–1×10^9 particles/ml.

If the sample is not monodisperse, then the decay constants tend to become systematically longer as the pair of experimental points, used to calculate the decay constant, increases in time. In addition, the average decay constants deviate from a linear dependence on $\sin^2 \theta/2$. Data of occasional virus samples showed large systematic deviations among the various calculated decay times and gross nonlinear angular dependence. Data from such samples were discarded.

Diffusion constants were calculated from the decay constants and then corrected to 20° assuming the validity of the Stokes–Einstein relation (Tanford, 1961)

$$D = kT/3\pi\eta_0 d \qquad (2)$$

where D is the diffusion constant; T the absolute temperature, k the Boltzman constant, η_0 the solvent viscosity, and d the diameter of the spheres. The viscosity was determined from published tables (Sober, 1970). This same expression was used to derive the hydrodynamic diameters. The sample temperatures were measured to within ±0.1°, and were stable within ±0.2° over the times required to record the autocorrelation functions. The Bausch and Lomb refractometer used to measure the index of refraction, and, therefore, the sucrose concentration, could be read to within ±0.0005 of a refractive index unit. For extensively dialyzed virus samples the uncertainty in the per cent sucrose concentrations was therefore about ±0.3% sucrose, which corresponds to an uncertainty in the viscosity of about ±1%. For virus samples suspended in high sucrose concentration, the uncertainty in viscosity was about ±2%.

Thus, the accumulated experimental error in determining the diffusion constant, and hence the derived hydrodynamic diameter, of one particular virus sample is estimated to be about ±3%. The averages over independent samples of the two types of virus are discussed later.

Figure 2 shows data for an AMV sample of concentration sufficiently low (2×10^7 particles/ml) that number fluctuations noticeably contribute to the correlation function. This spectrum was obtained in the course of a dilution series to estimate absolute concentration. Because the signal-to-noise ratio is low, and because of the obvious uncertainties in determining the base line of the diffusional terms for these dilute samples, we did not use them to measure diffusion constants. Thus angular dependent data are not shown in Figure 2. However, Figure 2 illustrates that even at these low concentrations, a reasonable determination of the diffusion constant is possible.

From the known volume of the virus sample prior to purification, we estimate that the virus concentration in the original plasma–citrate for MuLV and AMV were respectively 5.4×10^7 and 2.1×10^8 particles/ml. This is a lower limit, since some virus may be lost in purification.

b. Hydrodynamic Diameters. Figures 3 and 4 show the hydrodynamic diameters for a series of independent samples of AMV and MuLV in various solutions of sucrose and buffers. Several points deviate from the majority by amounts which exceed the estimated experimental uncertainty of the individual measurements. The cause of these deviations is not known, but as the points joined by lines in Figures 3 and 4 show, they are not reproduced when the same virus is resuspended in a different medium. This suggests that the deviations are associated with some random perturbation of the virus. Thus, if the average hydrodynamic diameters and diffusion constants are calculated from the linear average of all the points in each set then the statistical uncertainty estimated by the root mean square deviation of the set reflects the experimental uncertainties discussed above and possible variations intrinsic to the virus. For the diameters, these averages and uncertainties

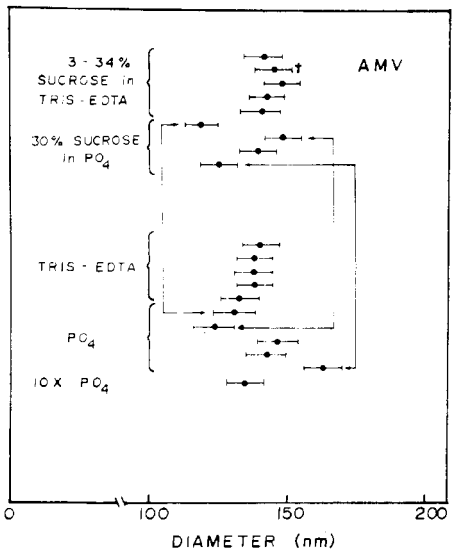

FIGURE 3: Hydrodynamic diameters for a number of samples of AMV in either 0.005 M phosphate (pH 7.01), denoted as PO_4 (10 × PO_4 = 0.05 M phosphate) or 0.005 M Tris-HCl-0.001 M EDTA (pH 8.1) denoted as Tris-EDTA. The error bars correspond to the experimental errors in the light scattering measurements as discussed in the text. The connected pairs of points correspond to the same sample in buffered sucrose and after removal of the sucrose by dialysis, as further discussed in the text. † refers to samples taken from a continuous sucrose gradient.

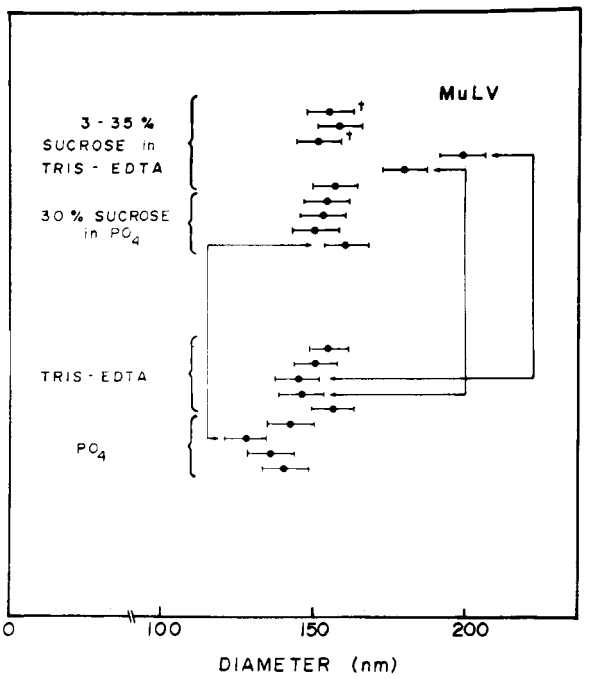

FIGURE 4: Same as Figure 3 for MuLV (Rauscher).

are: 138 ± 11 nm (AMV in sucrose); 138 ± 9 nm (AMV in sucrose-free buffer); 160 ± 13 nm (Rauscher in sucrose); and 144 ± 9 nm (Rauscher in sucrose-free buffer). If the deviant points are assumed to be spurious, and thus neglected in the averages, then the diameters are: 144 ± 3 nm (AMV in sucrose, neglecting the two smallest diameters); 138 ± 4 nm (AMV in buffer, neglecting the largest and smallest diameter); 154 ± 4 nm (Rauscher in sucrose, neglecting the two largest diameters); and 145 ± 6 nm (Rauscher in buffer, neglecting the smallest diameter). By neglecting these points, the statistical uncertainty among the samples is approximately that of a measurement on a single sample. We assume that the average determined by neglecting the deviant points is the best estimate from these data of the hydrodynamic diameters. These results are summarized in Table I.

c. Temperature Effects. In the process of budding from vertebrate cells, these viruses acquire a modified cell membrane. Because membrane structures are known to be temperature sensitive (Levine, 1972), the diameters of such viruses may be temperature dependent. Thus, we examined the temperature dependence and the results are summarized in Figure 5. Phosphate buffer was used in these measurements to avoid temperature dependent ionic strength and pH changes such as would occur with Tris-EDTA buffer for which the pK is temperature dependent. A slight temperature dependence over the range from 5 to 25° for viruses in sucrose was observed in two independent samples of each type of virus. The temperature dependence may be due to either specific changes in the virus caused by interactions with the sucrose, or to a failure of the Stokes-Einstein relation (eq 2). To test these alternatives, we measured the diameter of 176-nm polystyrene latex spheres as a function temperature both in sucrose and in water. The hydrodynamic diameter of these spheres in 20% sucrose was 175 ± 3 nm, and was independent of temperature in both sucrose and water. Therefore, we conclude that a high concentration sucrose solution is not a completely passive solvent for the virus. However, since the effect is small, no special emphasis is attributed to it at this time with regard to the physical properties of the viruses.

d. Measurements in Plasma-Citrate. An important

TABLE I: Hydrodynamic Properties and Sizes of MuLV and AMV.

	$D_{20,w}$ (× 10^7) (cm^2 sec^{-1})	Hydrodynamic Diameter (nm)	Particle Weight (daltons)	Volume % Water	Molecular Wt RNA	Electron Microscopy Diameter (nm)
MuLV in Tris or phosphate buffer	0.296 ± 0.012	145 ± 7	3.9×10^8	69	0.96×10^7	147[a]
MuLV in buffered sucrose	0.278 ± 0.005	154 ± 3[c]				
AMV in buffered sucrose	0.319 ± 0.007	144 ± 3[c]				
AMV in Tris or phosphate buffer	0.311 ± 0.009	138 ± 4	4.0×10^8	57	0.98×10^7	134–143[b]

[a] Luftig and Kilham (1971). [b] Luftig *et al.* (1974). [c] In 30% sucrose at 20°.

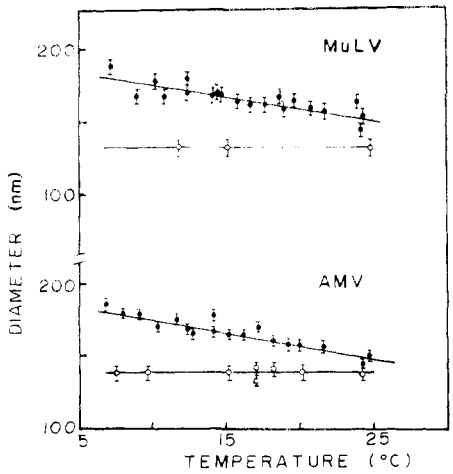

FIGURE 5: Temperature dependence of the hydrodynamic diameters of AMV and MuLV in buffered (0.005 M phosphate buffer, pH 7.01) sucrose and after removal of the sucrose by dialysis. ● 30.5% phosphate buffered sucrose; ○ phosphate buffer.

practical consideration is the extent to which RNA tumor viruses can be detected and characterized in natural fluids with a minimum of preparation. With this question in mind, we systematically examined plasma preparations from both virus producing and nonproducing mice.

For ten independent virus-free control mice, light scattering spectra were observed with decay constants which ranged from *ca.* 2.5×10^3 to 4.8×10^3 sec^{-1} (*cf.* the decay constant for purified MuLV of *ca.* 2.2×10^3 sec^{-1}). The corresponding scattered intensity varied widely among the controls with an average value that would approximate the result from a purified virus at a concentration of 5×10^8 particles/ml. The spectra from these controls indicated highly polydisperse material, as judged by both a threefold variation of the decay constant as calculated from various pairs of points on the experimental correlation function and by a highly nonlinear angular dependence.

We concluded that the study of viruses by this method in such a system would be possible only if virus concentrations exceeded 10^9 particles/ml. Accordingly, experiments on normal mouse plasma containing added purified MuLV to a concentration of 5×10^9 particles/ml yielded reasonably monodisperse data with a decay constant, corrected for the viscosity of plasma-citrate, equal to that observed for purified virus.

e. Sedimentation Coefficients. $s_{20,w}$ values for AMV and MuLV were found to be independent of concentration over the range of $3\text{–}7.5 \times 10^9$ particles/ml for AMV and $3\text{–}6.5 \times 10^8$ particles/ml for MuLV in the 0.005 M phosphate buffer. The $s_{20,w}$ values obtained for four different concentrations of each virus were 681 ± 30 for AMV and 625 ± 15 for MuLV. A $s_{20,w}$ value of 695 was obtained for AMV in the 0.005 M, pH 7.0 phosphate buffer containing 0.5 M KCl.

Discussion

a. Comparisons with Electron Microscopy. Comparisons of the hydrodynamic diameters with sizes determined by electron microscopy are difficult primarily because of the many variables involved in the preparation and interpretation of electron micrographs. Camerini-Otero *et al.* (1974) found, for a variety of bacteriophages and plant viruses, agreement (to at least 20%) between hydrodynamic diameters and those determined by electron microscopy, X-ray diffraction, and elastic light scattering. The diameters of RNA tumor viruses have been determined only by electron microscopy. Electron micrographs of various fixed preparations of AMV show particles with diameters of 80–160 nm (Bonar *et al.*, 1963), 107 nm (Gelderblom *et al.*, 1972), and 134–143 nm (Luftig *et al.*, 1974). In the judgement of Beard *et al.* (1963), the best estimate for the size of AMV is 120–140 nm. This is comparable with our value in sucrose-free buffer of 138 nm.

Diameters of particles in electron micrographs of MuLV have been reported as 95–125 nm (Zeigel and Rauscher, 1964), 90–100 nm (De Harven, 1968), 89–102 nm (Feller *et al.*, 1971), and 106–144 nm (Nermut *et al.*, 1972). The variability in these reported values may reflect in part the method of specimen preparation. For example, Nermut *et al.* (1972) obtained a value for MuLV of 106 nm after freeze-drying and shadowing, 130 nm for phosphotungstic acid negative staining followed by freeze-drying, and 144 nm after negative staining with uranyl acetate. Luftig and Kilham (1971), using catalase crystals as an internal size marker, reported a diameter of 147 nm. Considering well-known shrinkage problems in preparing samples for electron microscopy, this agrees surprisingly well with our hydrodynamic diameter of 145 nm measured in sucrose-free buffers. The agreement might be accounted for if one assumes that the fractional loss of water by the catalase crystals upon drying is comparable to that of the virus (Luftig, 1967). Since the known crystallographic repeat distance of wet catalase crystals is used as the scale, the virus diameter so obtained ought to be close to that of viruses in solution.

b. Particle Weights. From the measured diffusion and sedimentation constants, particle weights can be calculated according to the relation (Tanford, 1961)

$$M = RTs/D(1 - \bar{v}\rho) \qquad (3)$$

where R is the gas constant; T, the absolute temperature; D, the diffusion constant corrected to 20° and water; s, the sedimentation coefficient corrected to 20° and water; ρ, the density of the solvent, and $\bar{v}$ the partial specific volume of the particle. We used a value of $\bar{v}$ calculated by the method of Markham (1967). This method uses the viral composition recently calculated on a percentage basis by Stromberg *et al.* (1973) for AMV (61.5% protein, 2.4% RNA, 36.1% phospholipid) and summation of the partial specific volumes of the RNA, protein,, and lipid. We thus obtain a calculated $\bar{v}$ of 0.869. (The reciprocal of this gives a value of 1.15—in close agreement with the value of 1.16 deduced from the band position in the sucrose density gradient.) By employing this calculated $\bar{v}$, along with our experimentally determined values of $s_{20,w}$ and $D_{20,w}$, we calculate a molecular weight for AMV of 4.0×10^8. Our measured value for the AMV sedimentation constant, corrected to 20° and water, is 681 ± 30 S. We find a similar $s_{20,w}$ value of 695 in 0.5 M KCl. Sharp and Beard (1954) report a sedimentation constant for AMV in 0.55 M NaCl of 693 S, using a value of 0.772 for $\bar{v}$ as measured in D_2O. Adjustment of Sharp and Beard's value of 693 S to standard conditions using our value of $\bar{v}$ of 0.869, yields 688 S, which agrees well with our measured value at this higher ionic strength.

If we assume that MuLV has the same composition as AMV (and hence the same $\bar{v}$), using our value for the sedimentation coefficient of 625 ± 15 S we calculate a molecular weight of 3.9×10^8. Mora *et al.* (1966) report a molecular weight for MuLV virus of 2.2×10^8. However, in obtaining this value they used a sedimentation coefficient (ob-

tained in 0.18 M NaCl-0.02 M phosphate buffer (pH 7) containing 10^{-3} M magnesium chloride) of 640 S, which agrees well with our value of 625 ± 15 S, along with a diffusion constant calculated from the Stokes-Einstein relation (eq 2) using a diameter of 100 nm. The agreement between our determination of the MuLV sedimentation coefficient and that of Mora *et al.* (1966), despite the difference in salt concentration of the buffers utilized, indicates that use of the smaller viral diameter of 100 nm accounts for this lower molecular weight value.

From the estimated per cent composition of the macromolecular components and our values for the particle weights, we estimate that the molecular weight of the RNA is 0.94×10^7 for AMV and 0.96×10^7 for MuLV. This agrees well with the values of $1.0\text{-}1.2 \times 10^7$ for AMV (Robinson and Baluda, 1965; Huppert *et al.*, 1966) and $1.0\text{-}1.3 \times 10^7$ for MuLV (Mora *et al.*, 1966; Duesberg and Robinson, 1966).

c. Volume Fraction of Water. Since the buoyant density includes water bound by specific interactions, the particle weights estimated above include bound water, but not water which freely penetrates the virus particle (see, for example, Harrison, 1969). From the parameters reported in this paper, we can estimate the volume occupied by "free" water.

The particle volumes determined from the hydrodynamic diameters are: 14×10^{-16} cm^3 for AMV and 16×10^{-16} cm^3 for MuLV. The volume occupied by the macromolecular components together with specifically bound water is $M/A\rho$, where M is the particle weight determined above, A is Avagadro's number, and ρ is the particle density. These volumes are 6×10^{-16} and 5×10^{-16} cm^3 for AMV and MuLV, respectively. Thus, about 57% of the AMV and about 69% of the MuLV hydrodynamic volumes are occupied by "free" water. Sharp and Beard (1954) have estimated about 80% water for AMV; however, they obtained this estimate from their sedimentation data in D_2O and in bovine serum albumin solutions. Camerini-Otero *et al.* (1974) have used the same technique described here to estimate the volume fraction occupied by water for a number of bacteriophage and plant viruses. They find values in the range 52-65%, depending on the particular virus.

Acknowledgments

Our appreciation is expressed to Dr. J. L. Oncley for a critical discussion of this manuscript. We also thank Mr. Ernest Retzel for technical assistance with part of this work.

References

Bader, J. P. (1969), *in* The Biochemistry of Viruses, Levy, H. B. Ed., New York, N.Y., Marcel Dekker, pp 293-327.

Beard, J. W., Bonar, R. A., Heine, U., De Thé, G., and Beard, D. (1963), *in* Viruses, Nucleic Acids, and Cancer, Baltimore, Md., Williams and Wilkins, pp 344-373.

Benedek, G. B. (1968), *in* Polarization Matiére et Rayonnement, Livre de Jubilé en l'Honneur du Professeur A. Kastler, Paris, Presses Universitaires de France.

Bonar, R. A., and Beard, J. W. (1959), *J. Nat. Cancer Inst. 23,* 183-197.

Bonar, R. A., Heine, U., Beard, D., and Beard, J. W. (1963), *J. Nat. Cancer Inst. 30,* 949-997.

Camerini-Otero, R. D., Pusey, P. N., Koppel, D. E., Schaefer, D. W., and Franklin, R.M. (1974), *Biochemistry 13,* 960-970.

Clark, N. A., Lunacek, J. H., and Benedek, G. B. (1970), *Amer. J. Phys. 38,* 575-585.

De Harven, E. (1968), *in* Experimetal Leukemia, New York, N.Y., Appleton, pp 91-129.

Dubin, S. B., Benedek, G. B., Bancroft, F. C., and Freifelder, D. (1971), *J. Mol. Biol. 54,* 547-556.

Duesberg, P. H., and Robinson, W. S. (1966), *Proc. Nat. Acad. Sci. U. S. 55,* 219-227.

Feller, V., Dougherty, R. M., and Di Stefano, H. S. (1971), *J. Nat. Cancer Inst. 47,* 1289-1298.

Gelderblom, H., Bauer, H., Bolognesi, D. P., and Frank, H. (1972), *Zentralbl. Bakteriol., Parasitenk., Infektionskr. Hyg., Abt. 1, Orig. A 220,* 79-90.

Harrison, S. C. (1969), *J. Mol. Biol. 42,* 457-483.

Huppert, J., Lacour, F., Harel, J., and Harel, L. (1966), *Cancer Res. 26,* 1561-1568.

Koppel, D. W. (1971), *J. Appl. Phys. 42,* 3216-3225.

Levine, Y. K. (1972), *Progr. Biophys. Mol. Biol. 24,* 1-74.

Luftig, R. (1967), *J. Ultrastruct. Res. 20,* 91-102.

Luftig, R., and Kilham, S. S. (1971), *Virology 46,* 277-297.

Luftig, R. B., McMillan, P. N., Culbreth, K., and Bolognesi, D. P. (1974), *Cancer Res. 34,* 1694-1706.

Markham, R. (1967), *in* Methods in Virology, Vol. 2, Maramorosch, K., and Koprowski, H., Eds., New York, N.Y., Academic Press, pp 3-39.

Mora, P. T., McFarland, V. W., and Luborsky, S. W. (1966), *Proc. Nat. Acad. Sci. U. S. 55,* 438-445.

Nermut, M. V., Frank, H., and Schäfer, W. (1972), *Virology 49,* 345-358.

Pusey, P. N., Koppel, D. E., Schaefer, D. W., Camerini-Otero, R. D., and Koenig, S. H. (1974), *Biochemistry 13,* 952-960.

Rimai, L., Hickmott, J. T., Cole, T., and Carew, E. B. (1970), *Biophys. J. 10,* 20-37.

Robinson, W. S., and Baluda, M. A. (1965), *Proc. Nat. Acad. Sci. U. S. 54,* 1686-1692.

Salmeen, I. T., Gill, D., Rimai, L., McCormick, J. J., Maher, V. M., Arnold, W. J., and Hight, M. E. (1972), *Biochem. Biophys. Res. Commun. 47,* 1172-1178.

Schaefer, D. W., and Berne, B. J. (1972), *Phys. Rev. Lett. 28,* 475-477.

Schaffer, F. L., and Fromhagen, L. H. (1965), *Virology 25,* 662-664.

Sharp, D. G., and Beard, J. W. (1954), *Biochim. Biophys. Acta 14,* 12-17.

Sober, H. A. (1970), Handbook of Biochemistry, Cleveland, Ohio, Chemical Rubber Co., pp J-288-J-291.

Stromberg, K., Gantt, R., and Wilson, S. H. (1973), *Biochim. Biophys. Acta 304,* 1-11.

Tanford, C. (1961), Physical Chemistry of Macromolecules, New York, N.Y., Wiley.

Temin, N. W. (1971), *Annu. Rev. Biochem. 40,* 609-648.

Zeigel, R. F., and Rauscher, F. J. (1964), *J. Nat. Cancer Inst. 32,* 1277-1307.